Electronic Supporting Information

Aggregation induced emission (AIE) active 4-amino-1,8-naphthalimide-Tröger's base for the selective sensing of chemical explosives in competitive aqueous media

Jason M. Delente,[a,b] Deivasigamani Umadevi,[c] Sankarasekaran Shanmugaraju,*[d] Oxana Kotova,[a] Graeme W. Watson[c] and Thorfinnur Gunnlaugsson*[a,b]

[a]School of Chemistry and Trinity Biomedical Sciences Institute, Trinity College Dublin, The University of Dublin, Dublin 2, Ireland. E-mail: gunnlaut@tcd.ie

[b]AMBER (Advanced Materials and Bioengineering Research) Centre, Trinity College Dublin, The University of Dublin, Dublin 2, Ireland.

[c]School of Chemistry and Centre for Research on Adaptive Nanostructures and Nanodevices (CRANN), Trinity College Dublin, The University of Dublin, Dublin-2, Ireland.

[d]Chemistry, Indian Institute of Technology Palakkad (IITPKD), Kerala, India. E-mail: shanmugam@iitpkd.ac.in

---

Table of Contents: **Page No**

Experimental section

Materials and methods. All reagents, solvents, starting materials and nitroaromatic analytes were purchased from Sigma-Aldrich, Merck, or Fisher Scientific and were of reagent grade and were used as received. Solvents used were HPLC grade unless otherwise stated. Deuterated solvents ($(CD_3)_2SO$, $CDCl_3$, and CD_3CN) used for NMR analyses were purchased from Sigma-Aldrich or Apollo Scientific.

(***Caution!*** *Nitroaromatic analytes are classified as secondary chemical explosives and should be handled only in small quantity*)

The elemental analysis for C, H and N were performed on an Exeter analytical CE-450 elemental analyzer at University College Dublin (UCD).

FT-IR spectra were recorded in the range 4000-550 cm^{-1} on a Perkin-Elmer spectrometer equipped with a universal ATR sampling accessory.

The solution-phase ^{1}H and ^{13}C NMR spectra were recorded at 400 MHz and 101.2 MHz respectively using an Agilent Technologies 400-MR NMR spectrometer or recorded at 600 MHz and 150.8 MHz using a Bruker Avance II 600 NMR. Chemical shifts are reported in ppm with the deuterated solvents as the internal reference. All NMR spectra were carried out at 293 K.

Mass spectrometry was carried out using HPLC grade solvents. Electrospray mass spectra were determined on a Micromass LCT spectrometer and high-resolution mass spectra were determined relative to a standard of leucine enkephaline. Maldi Q-TOF mass spectra were carried out on a MALDI-Q-TOF-premier and high-resolution mass spectrometry was performed using Glu-Fib with an internal reference peak of *m/z* 1570.6774.

Morphology of **TBNap-TPy** was imaged using field emission scanning electron microscopy (FE-SEM) with an SE2 on the in-lens detector. The sample was prepared by drop-casting the DMSO or DMSO/Water mixture (4.79×10^{-6} M) of **TBNap-TPy** on silica wafers, then coated with Au and dried under vacuum before the imaging.

UV-visible absorption spectra were recorded in 1 cm quartz cuvettes (Hellma) on a Varian Cary 50 spectrometer. Baseline correction was applied for all spectra.

Emission spectra were recorded on a Varian Cary Eclipse Fluorimeter. The temperature was kept constant throughout the measurements at 298 K by using a thermostatic unit block.

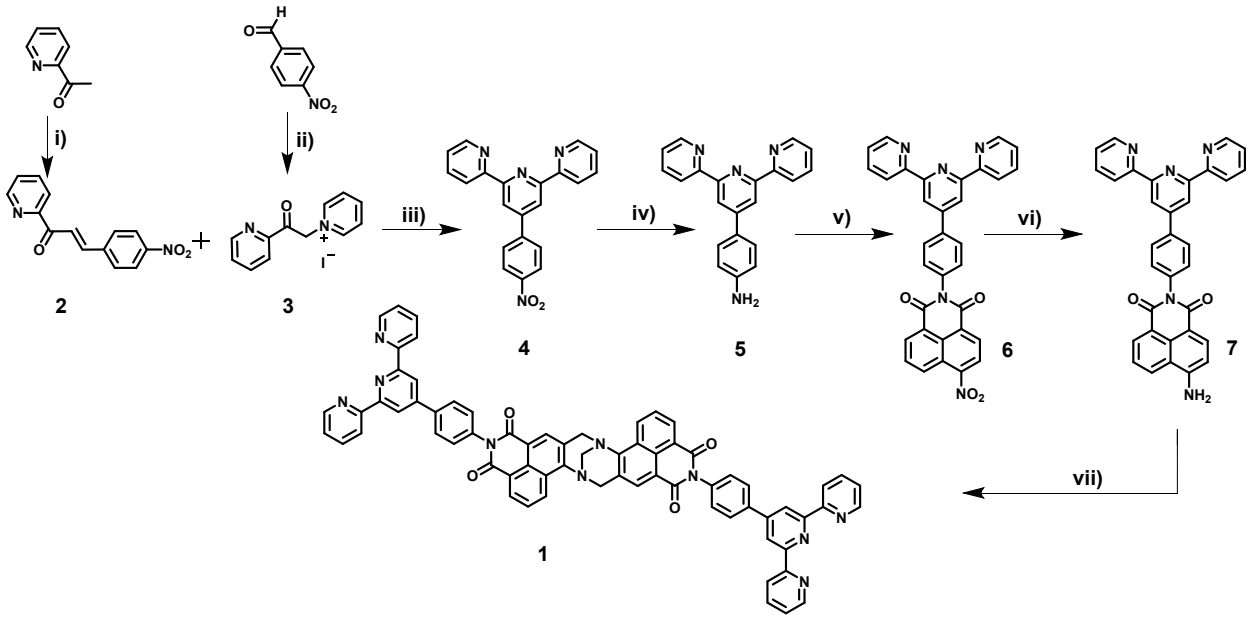

Scheme 1 : Synthesis of **TBNap-TPy** i) I_2, pyridine, Ar, reflux, 69%; ii) 2-acetylpridine, NaOH, MeOH, 32%; iii) NH_4OAc, MeOH, reflux 4 h, Ar, 75%; iv) 20% Pd/C, DMF, H_2, 24 h, 89%; v) 4-nitro-1,8-naphthalic anhydride, AcOH, reflux, 40%; vi) 20% Pd/C, DMF, H_2, 12 h, 95%; vii) paraformaldehyde, TFA, 79%.

Synthesis of (E)-3-(4-nitrophenyl)-1-(pyridine-2-yl)prop-2-en-1-one) (2):

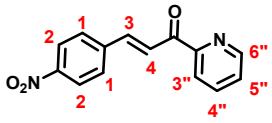

This compound was synthesized according to the procedure reported by Brudvig *et al.*[1] ^{1}H NMR spectrum was in good agreement with data previously reported in the literature.[1] ^{1}H NMR (400 MHz, $CDCl_3$, ppm) δ: 8.76 (1H, d, *J* = 4.4 Hz, $H_{6"}$), 8.43 (1H, d, *J* = 16.1 Hz, H_4), 8.27 (2H, d, J= 8.4 Hz, H_2), 8.20 (1H, d, J= 7.8 Hz, $H_{3"}$), 7.94 (1H, m, $H_{4"}$), 7.92 (1H, d, J=15.3 Hz, H_3), 7.86 (2H, d, J= 8.4 Hz, H_1), 7.53 (1H, m, $H_{5"}$).

Synthesis of (1-(2-oxo-2-(pyridine-2-yl)ethyl)pyridinium iodide (3):

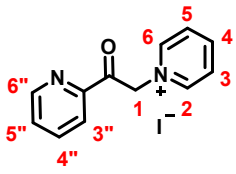

This compound was synthesized according to the procedure reported by Brudvig *et al.*[1] ^{1}H NMR spectrum was in good agreement with data previously reported in the literature.[2] ^{1}H NMR (400 MHz, CD_3CN, ppm) δ: 8.80 (1H, d, J= 4.8 Hz, $H_{6"}$), 8.73 (2H, d, J= 6.1 Hz, $H_{2,6}$), 8.64 (1H, t, J= 7.9 Hz, H_4), 8.13 (2H, t, J= 7.0 Hz, $H_{3,5}$), 8.07 (2H, m, $H_{4",3"}$), 7.74 (2H, t, J= 6.0 Hz, $H_{5"}$), 6.41 (2H, s, H_1).

Synthesis of (4′-(4-nitrophenyl)-2,2′:6′,2″-terpyridine) (4):

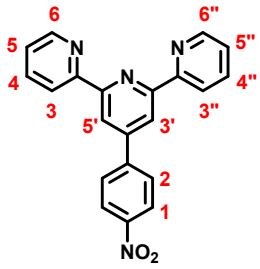

This compound was synthesized according to the procedure reported by Brudvig *et al.*[1] ^{1}H NMR spectrum was in good agreement with data previously reported in the literature.[1] ^{1}H NMR (600 MHz, DMSO-d_6, ppm) δ: 8.77 (2H, d, J= 6.4 Hz, $H_{6",6}$), 8.76 (2H, s, $H_{3',5'}$), 8.67 (2H, d, J= 7.9 Hz, $H_{3",3}$), 8.40 (2H, d, J= 8.7 Hz, H_1), 8.21 (2H, d, J= 8.7 Hz, H_2), 8.05 (2H, t, J= 7.8 Hz, $H_{4,4"}$), 7.54 (2H, dd, J= 6.9, 5.3 Hz, $H_{5",5'}$).

Synthesis of (4′-(4-aminophenyl)-2,2′:6′,2″-terpyridine)(5):

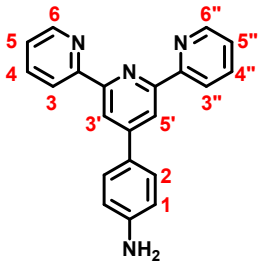

4′-(4-nitrophenyl)-2,2′:6′,2″-terpyridine (700 mg, 1.97 mmol) was reduced by catalytic hydrogenation using Pd/C (20%, 140mg) at 3 atm of H_2 in DMF (15 mL) for 24 h. The solution was filtered through a celite plug and washed several times with DMF. The solvent was removed under reduced pressure to isolate **5** (569 mg, 1.75 mmol, 89 %) as yellow solid after trituration in diethyl ether. ^{1}H NMR spectrum was in good agreement with data previously reported in the literature.[1] ^{1}H NMR (600 MHz, DMSO-d_6, ppm) δ: 8.75 (2H, d, J= 4.6 Hz, $H_{6",6}$), 8.64 (d, 2H, J= 8.1 Hz, $H_{3",3}$), 8.62 (s, 2H, $H_{3',3'}$), 8.02 (2H, t, J= 7.7 Hz, $H_{4",4}$), 7.67 (2H, d, J= 8.4 Hz, H_1), 7.50 (2H, m, $H_{5",5}$), 6.74 (2H, d, J= 8.4 Hz, H_1), 5.61 (s, 2H, NH_2).

Synthesis of 2-[4′-(4-aminophenyl)-2,2′:6′,2″-terpyridine]-4-nitro-1,8-naphthalimide (6, NitroNap-TPy):

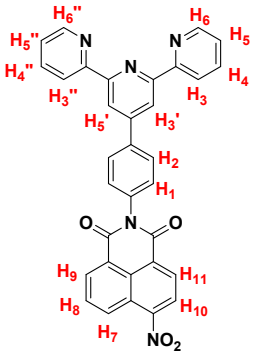

This synthesis was carried out according to modified literature procedure.[2-3] 4′-(4-aminophenyl)-2,2′:6′,2″-terpyridine (**5**, 200 mg, 0.616 mmol, 1 equiv.) and 4-nitro-1,8-naphthalic anhydride (150 mg, 0.616 mmol, 1 equiv.) were dispersed into acetic acid (15 mL) in a pressure vessel and the reaction mixture was refluxed for 24 h. After cooling down the mixture was poured into H_2O and the solution was basified to pH 6 using KOH leading to precipitation of beige solid. The precipitate was filtered and washed several times with water and cold methanol and diethyl ether. The solid was then triturated in ethyl acetate, filtered and washed with methanol and diethyl ether leading to the pure desired compound (132 mg, 0.204 mmol, 39 %). Melting Point = 307°C. HRMS (MALDI) Calculated for $C_{33}H_{20}N_5O_4$ m/z= 550.1515 $[M+H]^+$; Found m/z= 550.1532; ^{1}H NMR (600 MHz, DMSO-

d_6, ppm) δ : 8.81 (2H, s, $H_{3',5'}$), 8.79 (2H, d, J= 4.9 Hz, $H_{6,6''}$), 8.78 (m, 1H, H_9), 8.70 (2H, d, J= 7.9 Hz, $H_{3,3''}$), 8.69 (1H, d, J= 7.2 Hz, H_7), 8.66 (1H, d, J= 7.9 Hz, H_{11}), 8.61 (1H, d, J= 7.9 Hz, H_{10}), 8.15 (1H, dd, J= 8.3, 7.2 Hz, H_8), 8.14 (2H, d, J= 8.2 Hz, H_1), 8.06 (2H, td, J= 7.8, 1.6 Hz, $H_{4,4''}$), 7.66 (2H, d, J= 8.3 Hz, H_2), 7.55 (2H, dd, J= 7.0, 5.1 Hz, $H_{5,5''}$). ^{13}C NMR (150.8 MHz, DMSO-d_6, ppm): 163.8, 163.0, 156.3, 155.4, 149.9, 149.8, 149.4, 138.1, 138.0, 137.2, 132.2, 130.6, 130.6, 130.1, 129.4, 129.4, 128.1, 127.8, 125.1, 124.8, 123.9, 123.4, 121.5, 118.6. FTIR ν_{max} (cm^{-1}): 3058, 1716, 1673, 1585, 1524, 1214, 1467, 1441, 1415, 1389, 1369, 1344, 1339, 1235, 1193, 1134, 1122, 1077, 1040, 988, 914, 858, 825, 783, 780, 757, 738, 711, 695.

Synthesis of 2-[4′-(4-aminophenyl)-2,2′:6′,2″-terpyridine]-4-amino-1,8-naphthalimide (7, AminoNap-TPy):

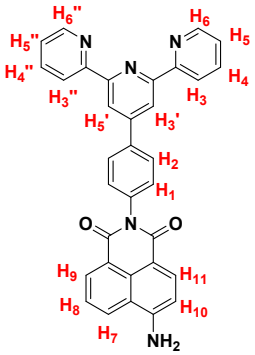

This synthesis was carried out according to modified literature procedure.[4] 2-[4′-(4-aminophenyl)-2,2′:6′,2″-terpyridine]-4-nitro-1,8-naphthalimide (**6**,122 mg, 0.222 mmol) was reduced by catalytic hydrogenation using Pd/C (20%, 25mg) at 3 atm of H_2 in DMF (15 mL) overnight. The mixture was diluted in 60 mL of EtOH, filtered through a celite plug and washed several times with DMF. The solvent was removed under reduced pressure to isolate **7** (110 mg, 0.212 mmol, 95 %) as mustard solid after trituration in diethyl ether. Melting Point = 329°C. HRMS (ESI^-) Calculated for $C_{33}H_{20}N_5O_2$ m/z = 518.1622 $[M-H]^-$. Found m/z = 518.1616. ^{1}H NMR (600 MHz, DMSO-d_6, ppm) δ : 8.80 (2H, s, $H_{3',5'}$), 8.79 (2H, d, J= 4.2 Hz $H_{6,6''}$), 8.70 (2H, d, J= 8.0 Hz, $H_{3,3''}$), 8.69 (1H, d, J= 8.8 Hz, H_7), 8.47 (1H, d, J= 7.1 Hz, H_9), 8.23 (1H, d, J= 8.23 Hz, H_{11}), 8.08 (2H, d, J= 8.3 Hz, H_2), 8.06 (2H, m, $H_{4,4''}$), 7.71 (1H, t, J= 7.8 Hz, H_8), 7.55 (2H, m, $H_{5,5''}$), 7.54 (2H, m, H_1), 6.90 (1H, d, J= 8.3 Hz, H_{10}). ^{13}C NMR (150.8 MHz, DMSO-d_6, ppm): 164.1, 163.2, 155.8, 155.0, 153.0, 149.4, 149.0, 137.9, 137.5, 137.0, 134.1, 131.2, 130.4, 130.3, 129.6, 127.4, 124.6, 124.1, 122.2, 121.0, 119.6, 118.1. FTIR ν_{max} (cm^{-1}): 3470, 3316, 3160, 1690, 1650, 1584, 1518, 1466, 1363, 1345, 1234, 1133, 1130, 990, 914, 887, 822, 793, 772, 740, 694, 659.

Synthesis of Bis-2-[4′-(4-aminophenyl)-2,2′:6′,2″-terpyridine]-4-amino-1,8-naphthalimide-[b,f][1,5]-diazocine (1, TBNap-TPy):

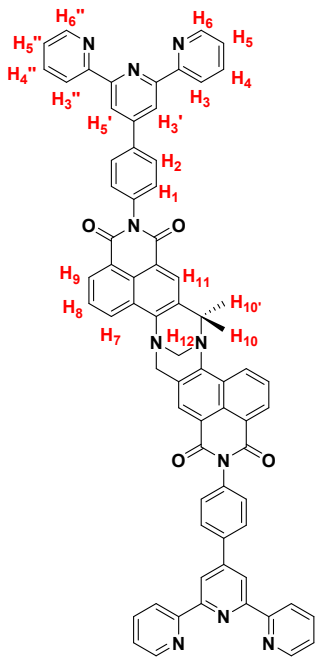

This synthesis was carried out according to modified literature procedure.[4] 2-[4′-(4-aminophenyl)-2,2′:6′,2″-terpyridine]-4-amino-1,8-naphthalimide (200 mg, 0.385 mmol, 1 equiv.) and paraformaldehyde (17.3 mg, 0.577 mmol, 1.5 equiv.) were flushed with argon. Trifluoroacetic acid (4 mL) was added at 0 °C and the solution was stirred at room temperature overnight under inert atmosphere. The mixture was added dropwise to a solution of aqueous ammonia at 0 °C. DCM was added and the organic phase was washed with $NaHCO_3$ saturated solution followed by H_2O. The organic phase was dried over $NaSO_4$ and the solvent was removed under reduced pressure. The solid was triturated in diethyl ether and isolated *via* filtration as an orange solid (125 mg, 0.116 mmol, 77 %). Melting Point = 308°C. Elemental analysis calculated for $C_{69}H_{42}N_{10}O_4 \cdot 0.13CH_3Cl \cdot 0.01DMF \cdot 1.9H_2O$: C, 73.79; H, 4.12; N, 12.45; Found: C, 73.80; H, 3.84; N, 12.35. HRMS (MALDI) Calculated for $C_{69}H_{43}N_{10}O_4$ m/z = 1075.3469 $[M+H]^+$ Found m/z = 1075.3445. ^1H NMR (600 MHz, DMSO-d_6, ppm) δ : 8.79 (2H, d, J = 8.4 Hz, H_9), 8.77 (4H, m, $H_{6,6"}$), 8.77 (4H, s, $H_{3',5'}$), 8.69 (4H, d, J= 7.9 Hz, $H_{3,3"}$), 8.52 (2H, d, J= 7.2 Hz, H_7), 8.19 (2H, s, H_{11}), 8.06 (4H, m, H_2), 8.05 (4H, m, 4H, $H_{4,4"}$), 8.00 (2H, t, J= 7.9 Hz, H_8), 7.54 (8H, m, H_1 and $H_{5,5"}$), 5.23 (2H, d, J= 17.6 Hz, H_{10}), 4.79 (2H, s, H_{12}), 4.74 (2H, d, J= 17.6Hz, $H_{10'}$). ^{13}C NMR (150.8 MHz, DMSO-d_6, ppm): 163.7, 163.2, 155.8, 154.9, 149.4, 149.3, 148.9, 137.5, 137.3, 137.2, 130.7, 130.4, 130.2, 129.4, 128.0, 127.5, 127.2, 126.8, 126.2, 124.6, 123.0, 121.0, 118.2, 118.1, 64.9, 56.9. FTIR ν_{max} (cm^{-1}): 3063, 1705, 1665, 1584, 1567, 1512, 1467, 1459, 1404, 1369, 1339, 1301, 1240, 1177, 1127, 1087, 1034, 991, 928, 891, 830, 815, 783, 774, 737, 688, 659.

Preparation of the solution of TBNap-TPy for aggregation-induced emission: A solution of **TBNap-TPy** was prepared by dissolving 10.3 mg of the compound into 20 mL of DMSO. Then dilution with the desired amount of DMSO was done and a precise volume of deionized water was added if necessary to reach the desired percentage of water in solution with a final concentration of 4.8 x 10^{-6} M. For all the emission measurements, the excitation wavelength was λ_{ex} = 388 nm and the emission spectrum were recorded in the range of λ_{em} = 400-800 nm.

Preparation of Nitroaromatics Solutions:

***(Caution!** Nitroaromatic analytes are classified as secondary chemical explosives and should be handled only in small quantity)* The desired quantity of each of the nitroaromatics was dissolved into 14 mL of spectroscopic grade DMSO and then 6 mL of deionized water was slowly added to the solution.

Fluorescence titration experiments: Every time a freshly prepared solution of **TBNap-TPy** (4.8×10^{-6} M) was used. During the fluorescence titration, 1 mM solution of different nitroaromatic explosives was added (0.0 μM ─74.1 μM) in an incremental fashion (20 μL each addition). The emission intensity was monitored after each addition. For all the fluorescence titration experiments, the excitation wavelength was 388 nm and the emission spectra were recorded in the range of 400-800 nm. The percentage of quenching efficiency was calculated from the following equation:

$$\text{Quenching efficiency (\%)} = (I_0\text{-}I)/I_0 \times 100$$

Where I_0 is the initial emission intensity of **TBNap-TPy** in DMSO: H_2O (70:30) and I is the intensity after the addition of the analyte.

Computational methods and model: All the calculations were done by using the Minnesota M06-2X[5] functional and the 6-311G(d,p) basis set. All the calculations were done by using Gaussian 09 package.[6] The M06-2X method was chosen, as it has been shown to be better when compared to the more popular B3LYP alternatives when modeling nonbonding interactions.[7] The model system used to represent **TBNap-TPy** is shown in Fig. S36. Binding energy (BE) was calculated as the difference between the sum of the total energies of **TBNap-TPy** (E_{TB}) and Picric acid (E_{PA}) and the total energy of the complex(E_{TB+PA}) as given in the equation below,

$$BE = (E_{TB} + E_{PA}) - E_{TB+PA}$$

The binding energy was corrected for basis set superposition error (BSSE) using the counterpoise correction method.

References:

1 (a) A. C. L. Durrell, Gonghu; Koepf, Matthieu; Young, Karin J.; Negre, Christian F A; Allen, Laura J.; McNamara, William R.; Song, Hee Eun; Batista, Victor S.; Crabtree, Robert H.; Brudvig, Gary W, *Journal of Catalysis*, 2014, **310**, 37; (b) P. C. Mondal and A. K. Manna, *New J. Chem.*, 2016, **40**, 5775.

2. J. Wang, M. Pappalardo and F. Keene, *Aust. J. Chem.*, 1995, **48**, 1425.

3. J. I. Lovitt, C. S. Hawes, A. D. Lynes, B. Haffner, M. E. Möbius and T. Gunnlaugsson, *Inorganic Chemistry Frontiers*, 2017, **4**, 296.
4. S. Shanmugaraju, C. Dabadie, K. Byrne, A. J. Savyasachi, D. Umadevi, W. Schmitt, J. A. Kitchen, and T. Gunnlaugsson, *Chem. Sci.*, 2017, **8**, 1535.

5. Y. Zhao and D. G. Truhlar, *Theor. Chem. Acc*., 2008, **120**, 215.

6. Gaussian 09, Revision A.02, M. J. Frisch, G. W. Trucks, H. B. Schlegel, G. E. Scuseria, M. A. Robb, J. R. Cheeseman, G. Scalmani, V. Barone, G. A. Petersson, H. Nakatsuji, X. Li, M. Caricato, A. Marenich, J. Bloino, B. G. Janesko, R. Gomperts, B. Mennucci, H. P. Hratchian, J. V. Ortiz, A. F. Izmaylov, J. L. Sonnenberg, D. Williams-Young, F. Ding, F. Lipparini, F. Egidi, J. Goings, B. Peng, A. Petrone, T. Henderson, D. Ranasinghe, V. G. Zakrzewski, J. Gao, N. Rega, G. Zheng, W. Liang, M. Hada, M. Ehara, K. Toyota, R. Fukuda, J. Hasegawa, M. Ishida, T. Nakajima, Y. Honda, O. Kitao, H. Nakai, T. Vreven, K. Throssell, J. A. Montgomery, Jr., J. E. Peralta, F. Ogliaro, M. Bearpark, J. J. Heyd, E. Brothers, K. N. Kudin, V. N. Staroverov, T. Keith, R. Kobayashi, J. Normand, K. Raghavachari, A. Rendell, J. C. Burant, S. S. Iyengar, J. Tomasi, M. Cossi, J. M. Millam, M. Klene, C. Adamo, R. Cammi, J. W. Ochterski, R. L. Martin, K. Morokuma, O. Farkas, J. B. Foresman, and D. J. Fox, Gaussian, Inc., Wallingford CT, 2016.

7. M. Walker, A. J. A. Harvey, A. Sen, and C. E. H. Dessent, *J. Phys. Chem. A* 2013, **117**, 47, 12590.

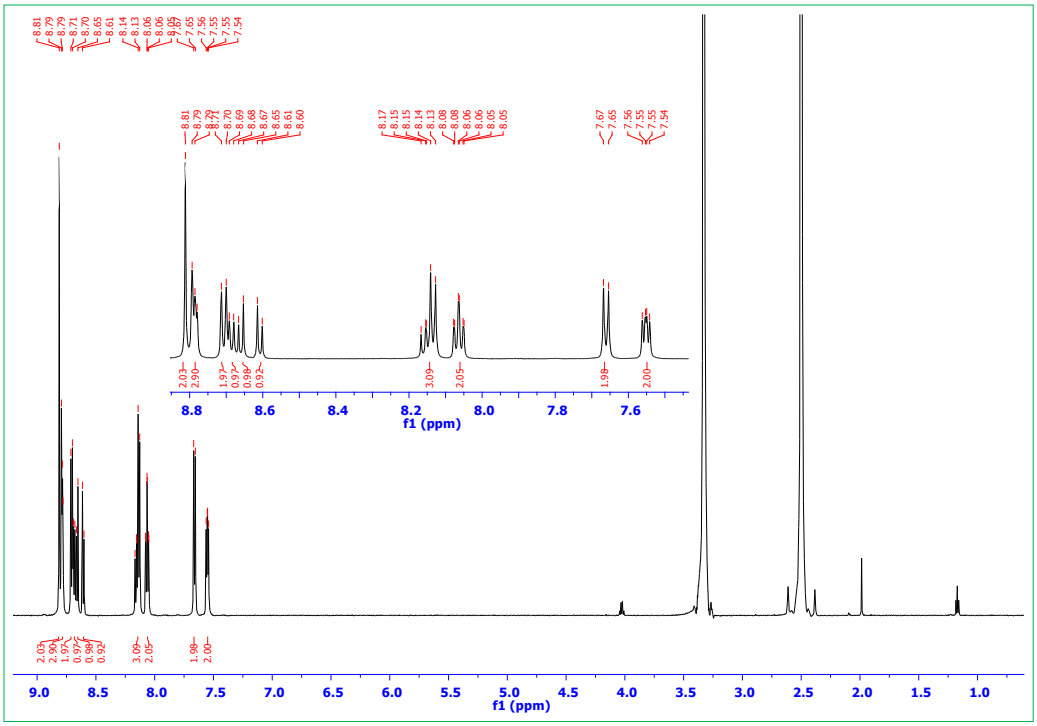

Fig. S1. ^{1}H NMR (600 MHz, DMSO-d_6) of **NitroNap-TPy**.

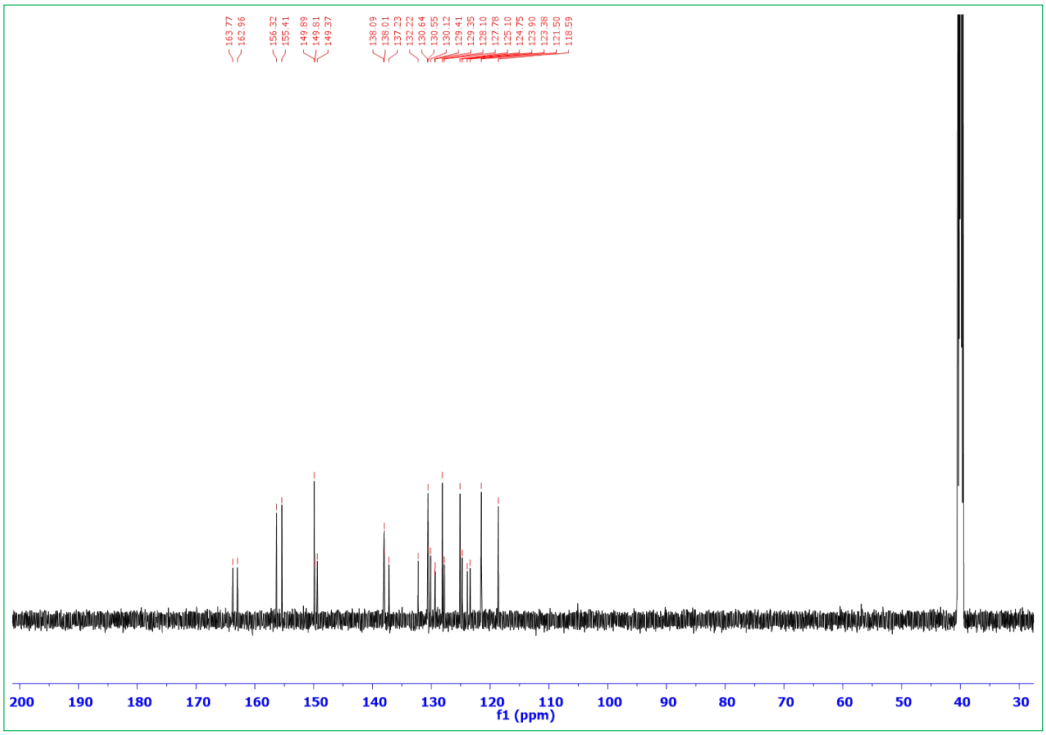

Fig. S2. ^{13}C NMR (150.8 MHz, DMSO-d_6) of **NitroNap-TPy**.

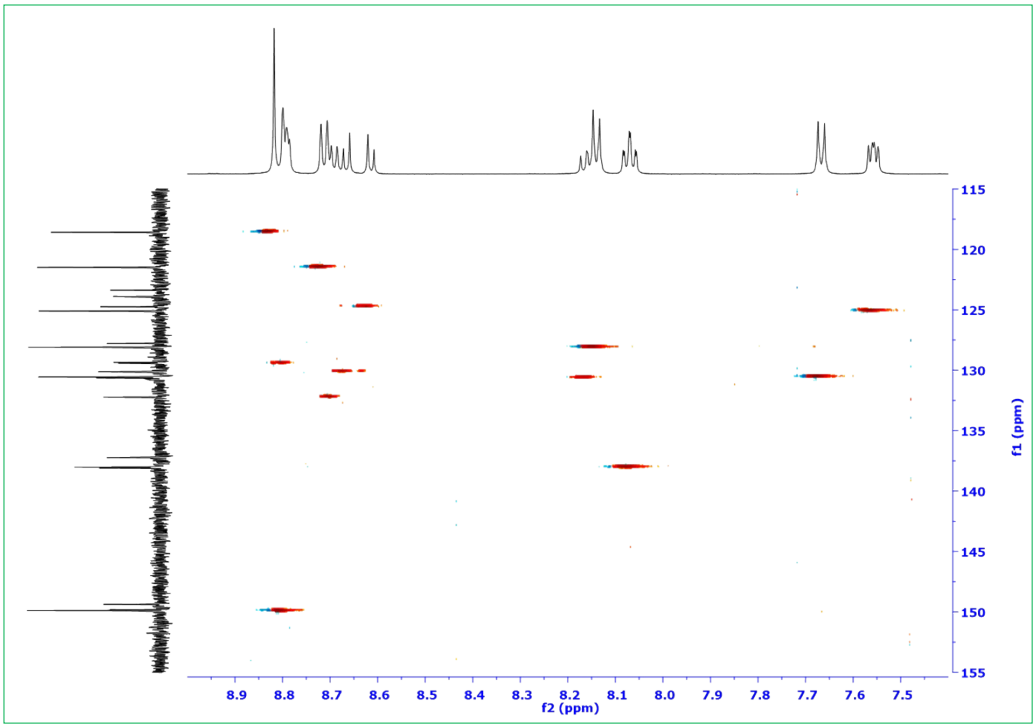

Fig. S3. HSQC NMR of **NitroNap-TPy**.

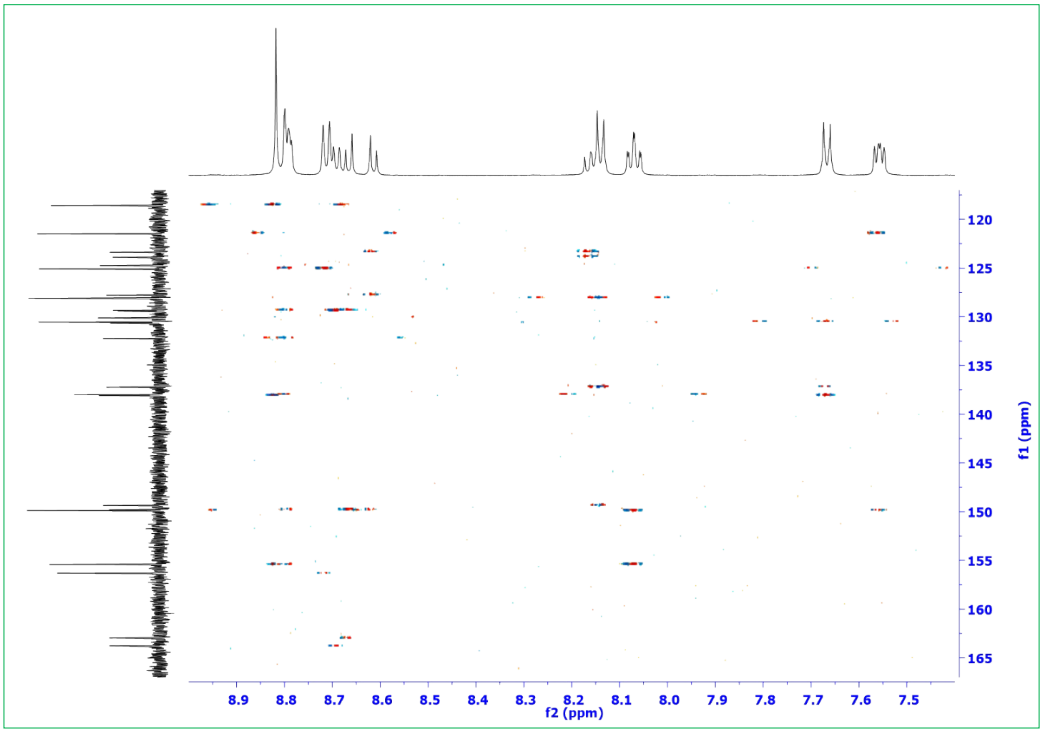

Fig. S4. HMBC NMR of **NitroNap-TPy**.

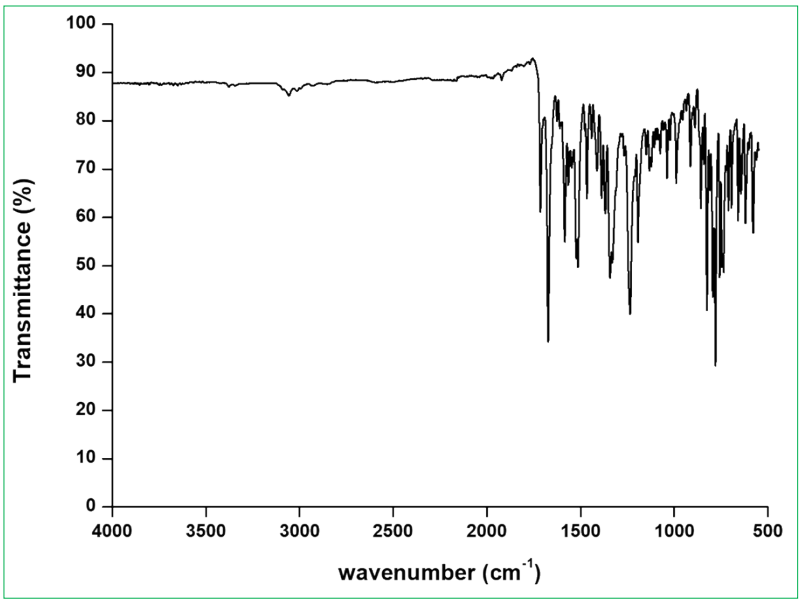

Fig. S5. IR spectrum of **NitroNap-TPy**.

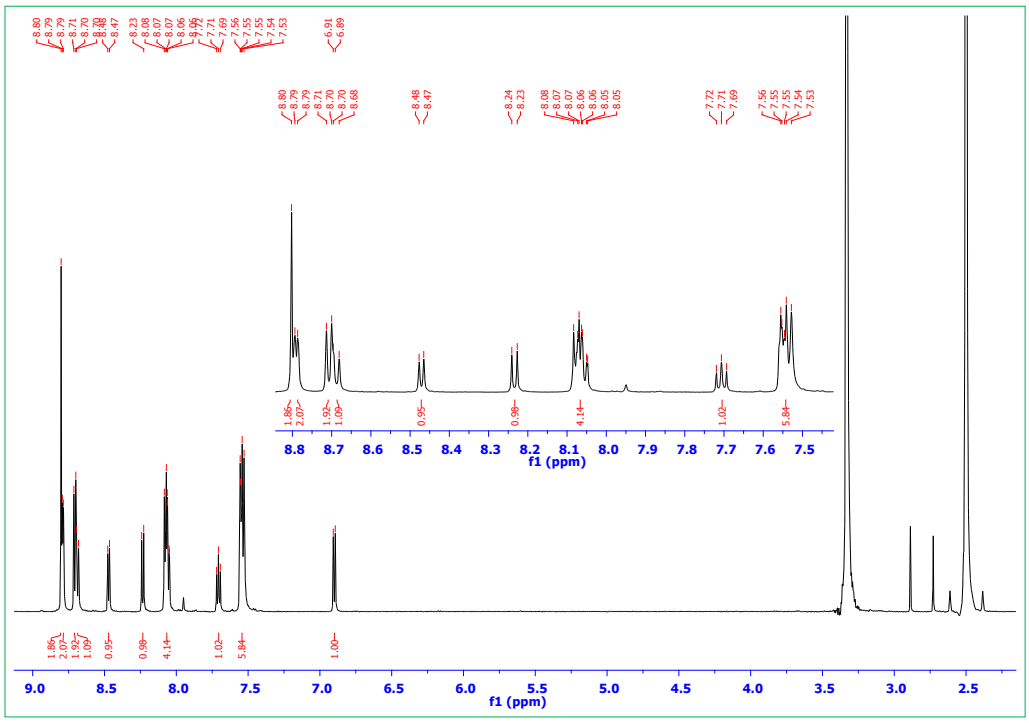

Fig. S6. ^{1}H NMR (600 MHz, DMSO-d_6) of **AminoNap-TPy**.

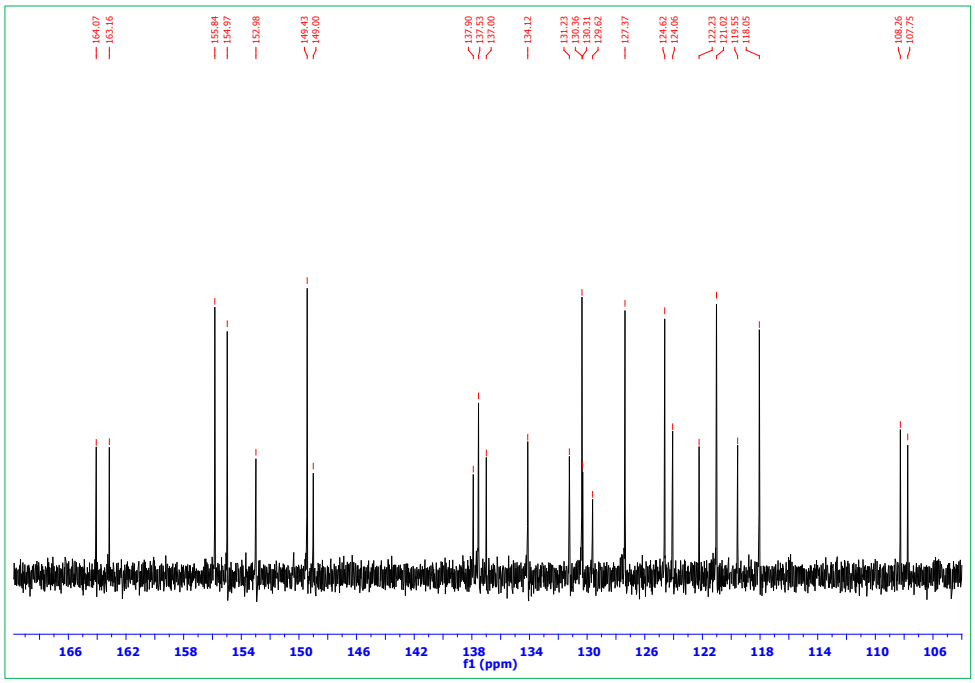

Fig. S7. ^{13}C NMR (150.8 MHz, DMSO-d_6) of **AminoNap-TPy**.

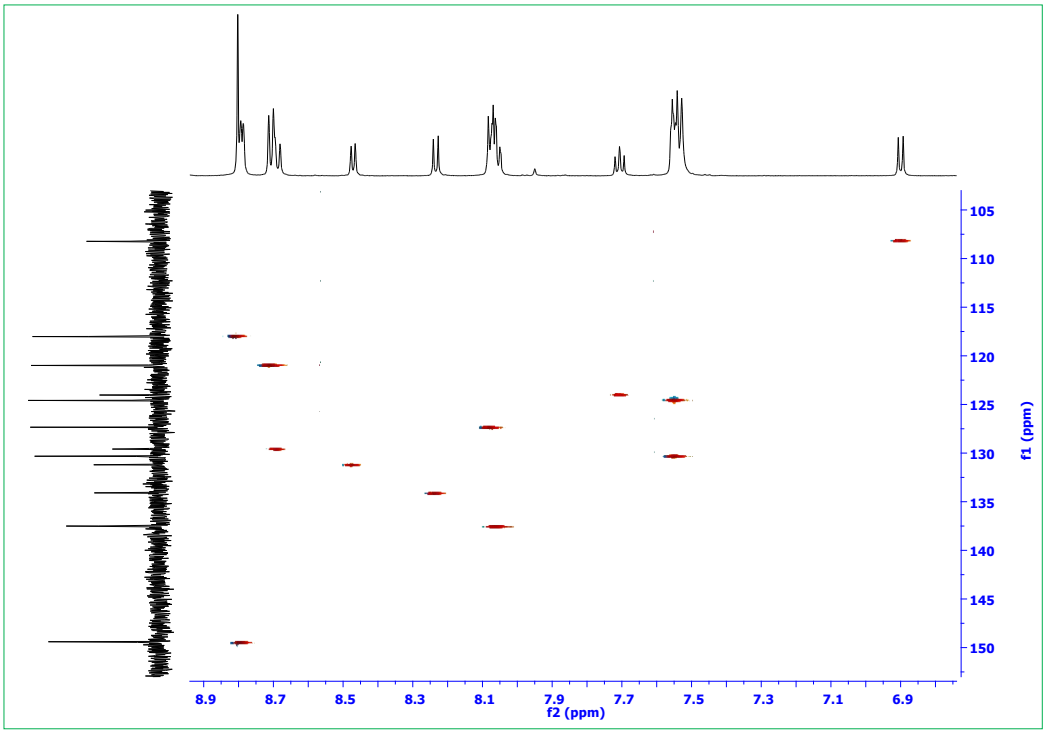

Fig. S8. HSQC NMR of **AminoNap-TPy**.

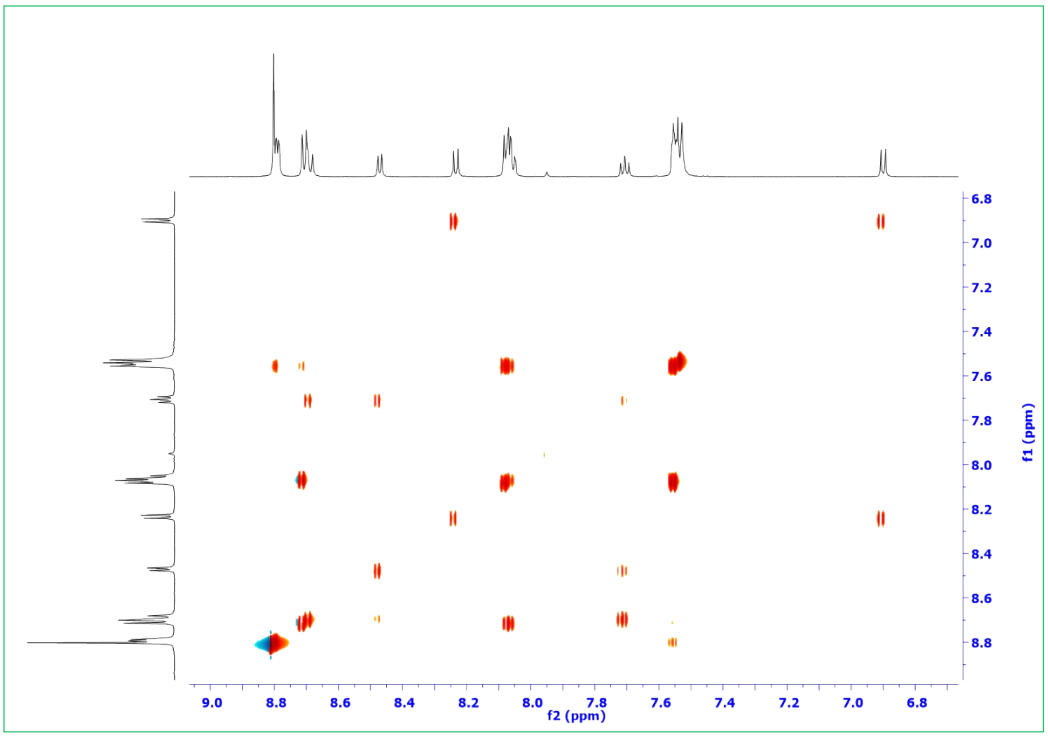

Fig. S9. HH COSY of **AminoNap-TPy**.

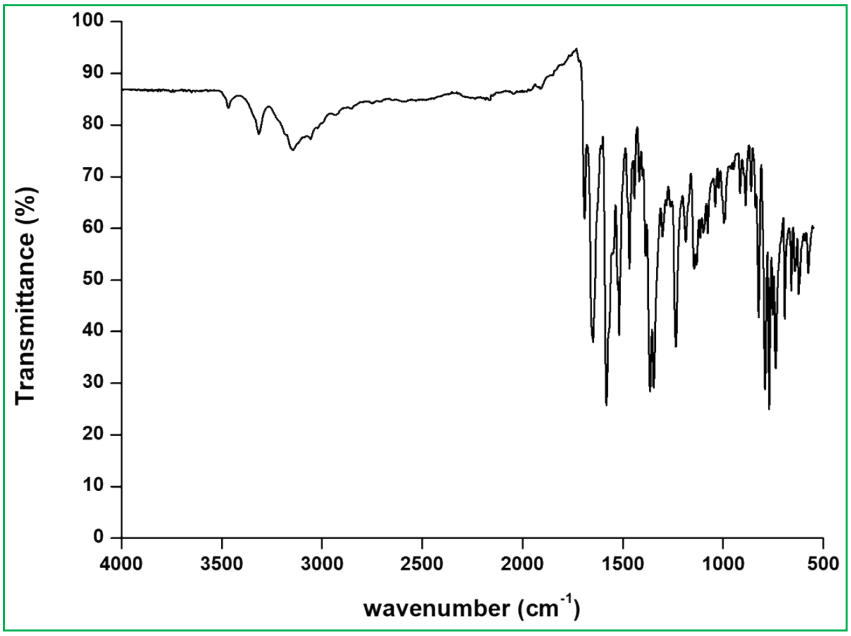

Fig. S10. IR Spectrum of **AminoNap-TPy**.

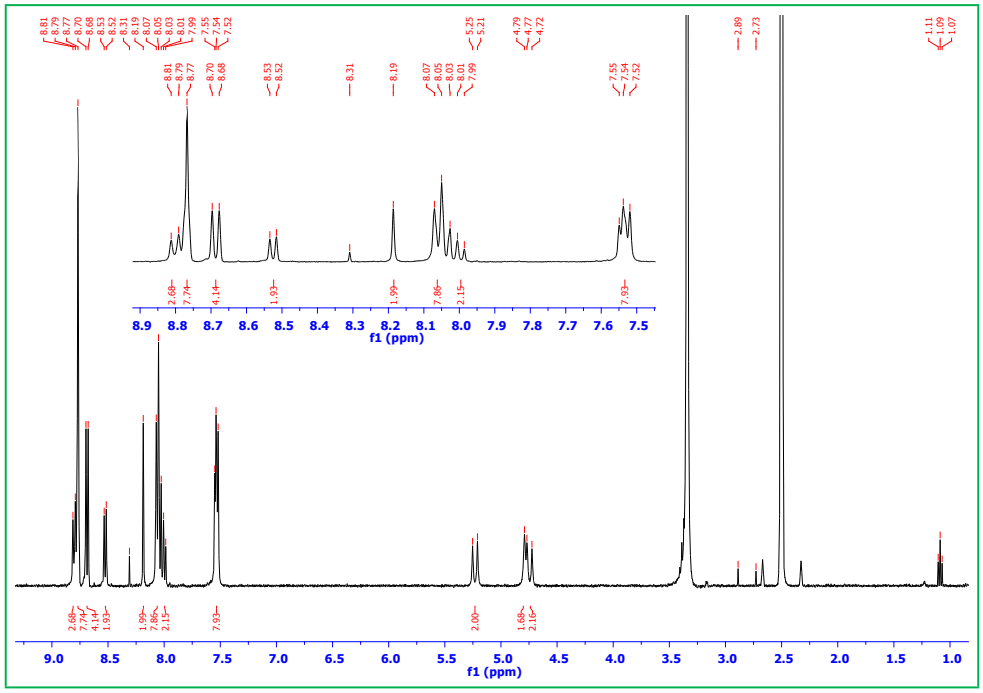

Fig. S11. ^{1}H NMR (600 MHz, DMSO-d_6) of as-synthesized **TBNap-TPy**.

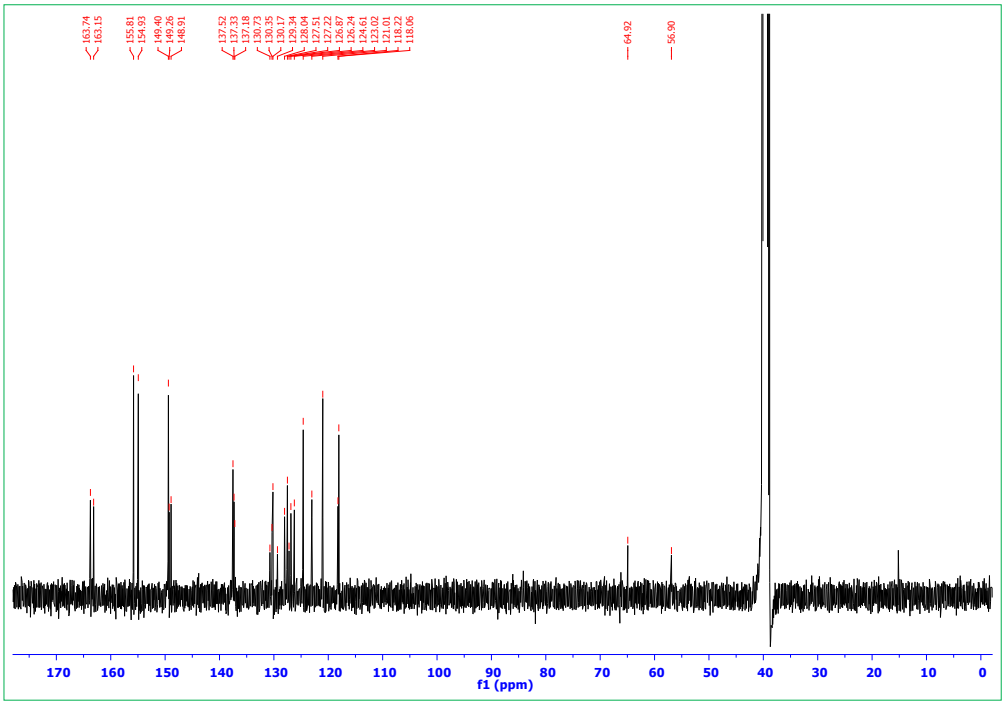

Fig. S12. ^{13}C NMR (150.8 MHz, DMSO-d_6) of **TBNap-TPy**.

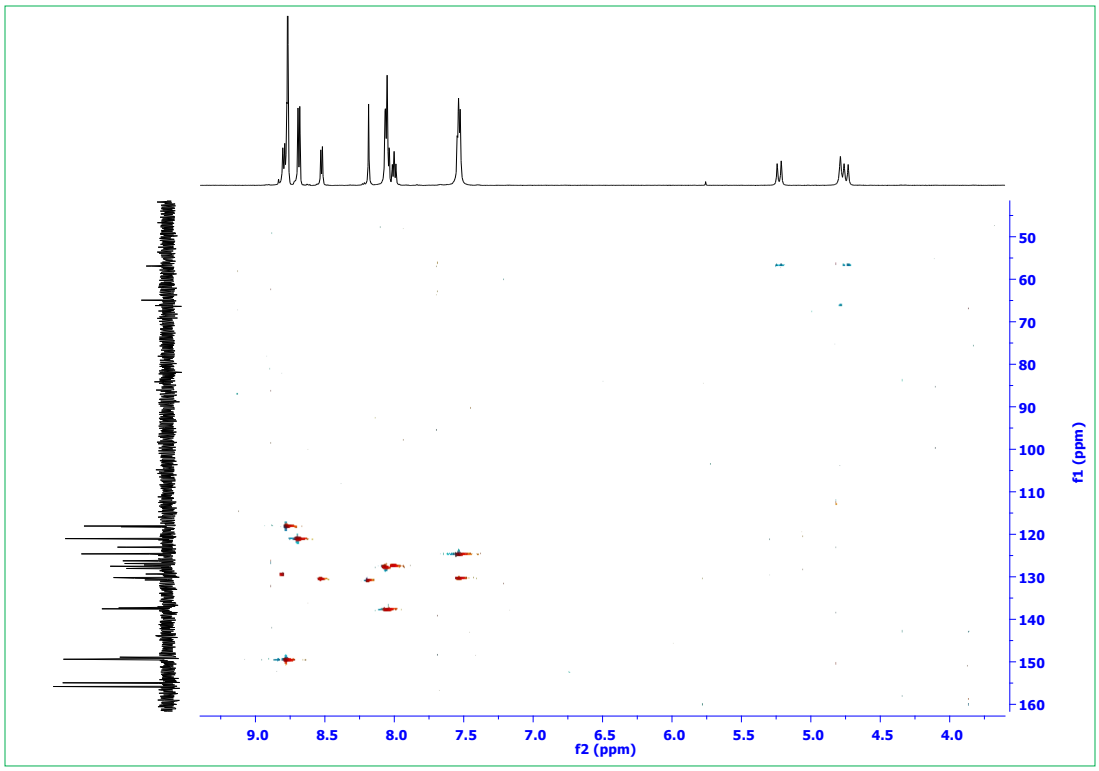

Fig. S13. HSQC NMR of **TBNap-TPy**.

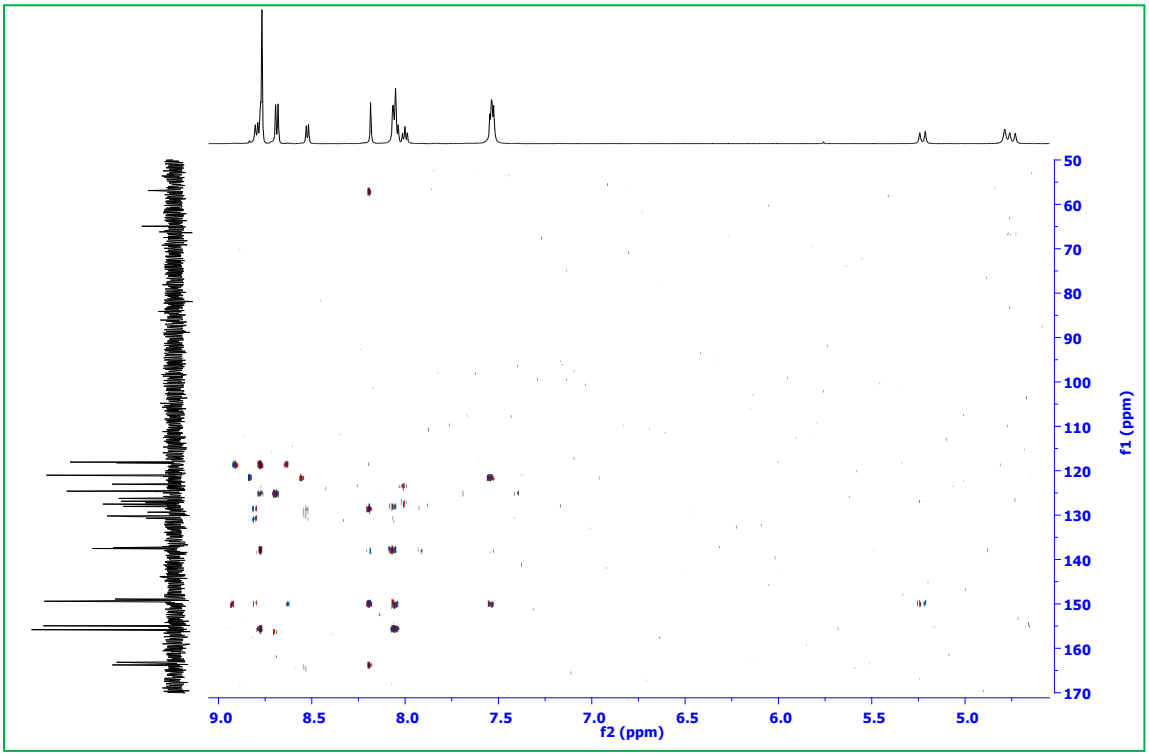

Fig. S14. HMBC NMR of **TBNap-TPy**.

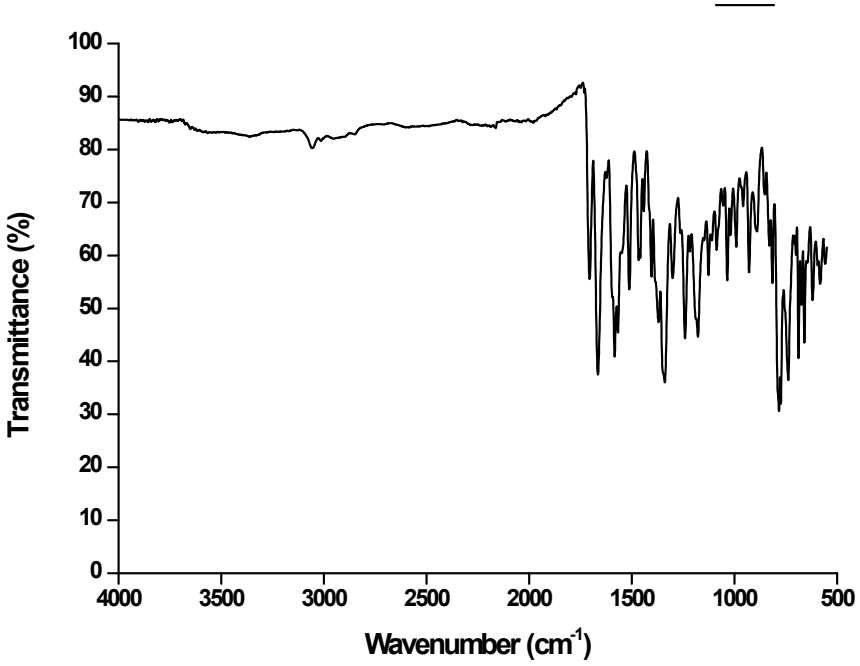

Fig. S15. The FT-IR spectrum of **TBNap-TPy**.

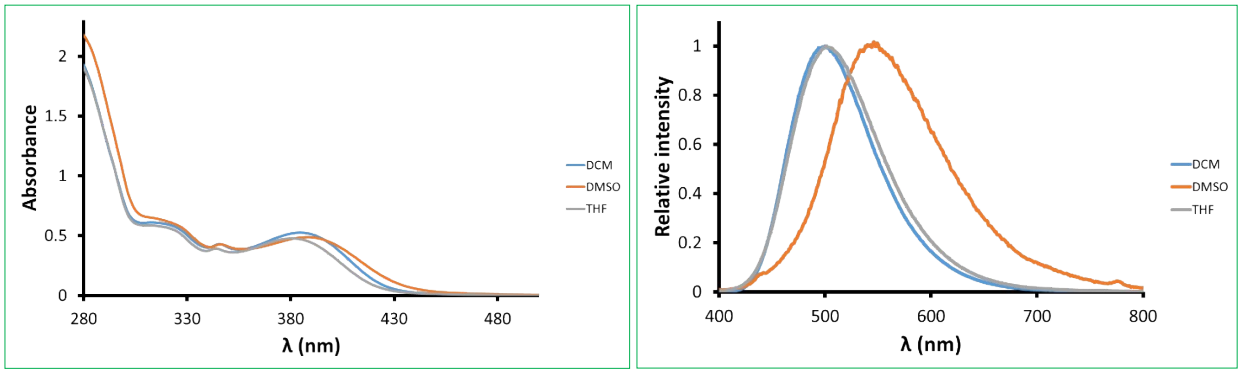

Fig. S16. Absorbance spectra (left) and normalized emission spectra (right) of **TBNap-TPy** in DCM, DMSO, THF. (c= 2.5×10^{-5} M), λ_{exc}= 388 nm for DCM and DMSO, λ_{exc}= 380 nm for THF.

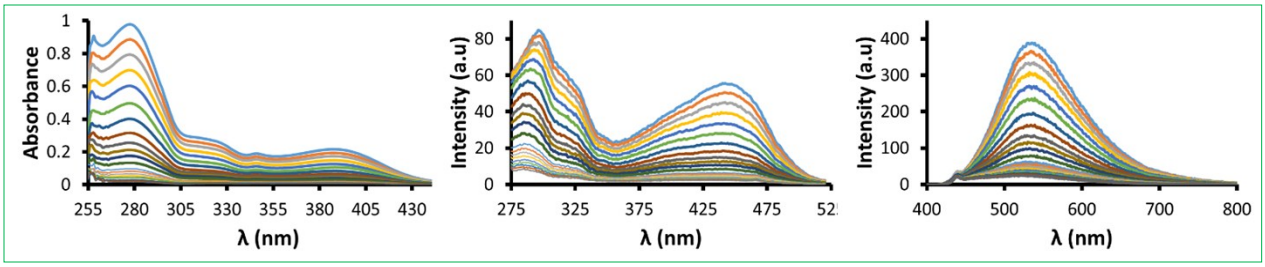

Fig. S17. Absorbance spectra (left) excitation spectra (middle) and emission spectra (right) of **TBNap-TPy** in DMSO. (c = 1.0 x10^{-5} M to c = 2.6 x10^{-7} M), λ_{exc}= 388 nm.

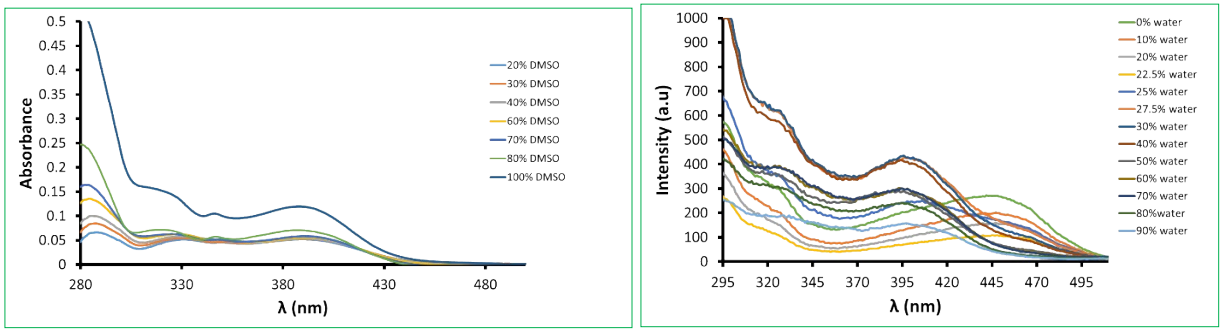

Fig. S18. Absorbance spectra (left) and excitation spectra (right) of **TBNap-TPy** in DMSO (c= 4.6x10^{-6} M) at different percentage of water content.

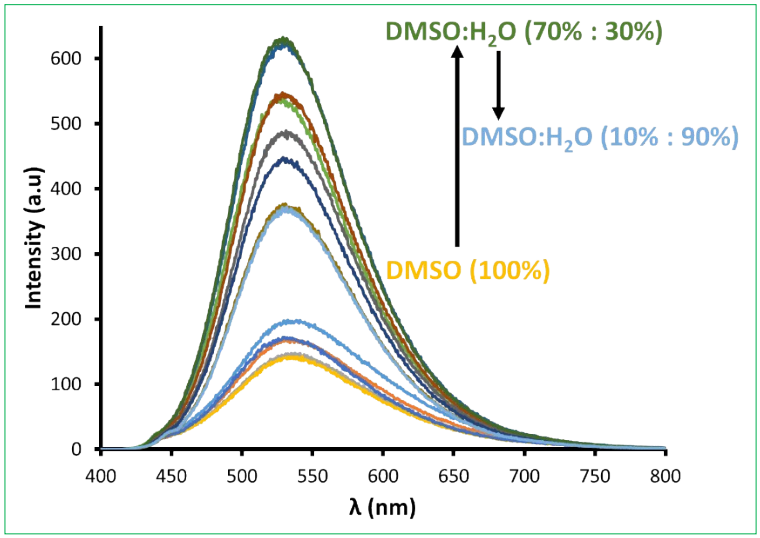

Fig. S19. The emission spectrum of **TBNap-TPy** in DMSO (c = 4.6 x 10^{-6} M) at different percentages of water content.

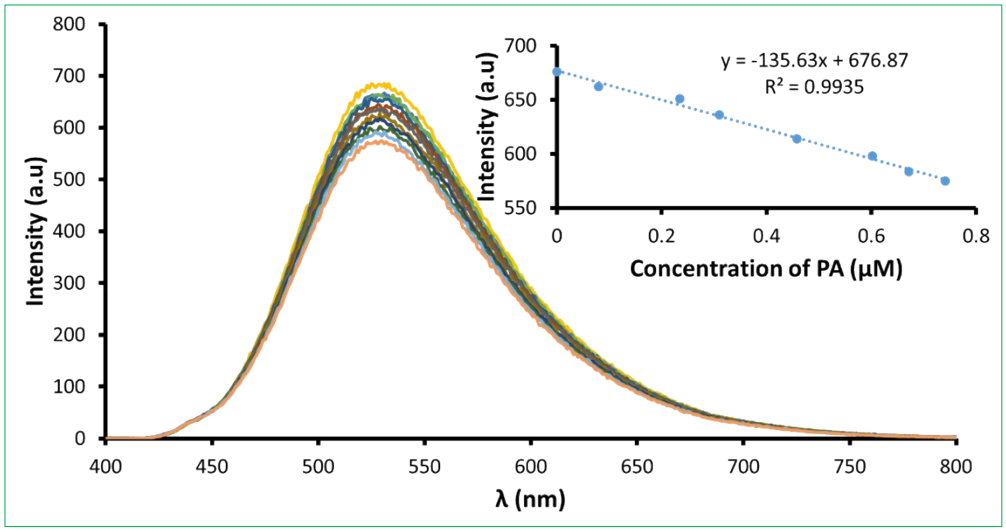

Fig. S20. Sensitivity experiment of **TBNap-TPy** in DMSO-H_2O (70-30) (c= $4.6x10^{-6}$ M) in presence of PA (0-0.74 μM).

The limit of detection for PA in DMSO-H_2O (70-30) was calculated using the following equation:

$$\textbf{Limit of detection} = 3\sigma/K = 8.75 \times 10^{-8}\ \textbf{mol.L} = \textbf{20.0 ppb}$$

Where σ (3.95) is the standard deviation of the initial emission intensity of **TBNap-TPy** in DMSO: H_2O (70:30) before the addition of PA and *K* is the slope of the linear curve.

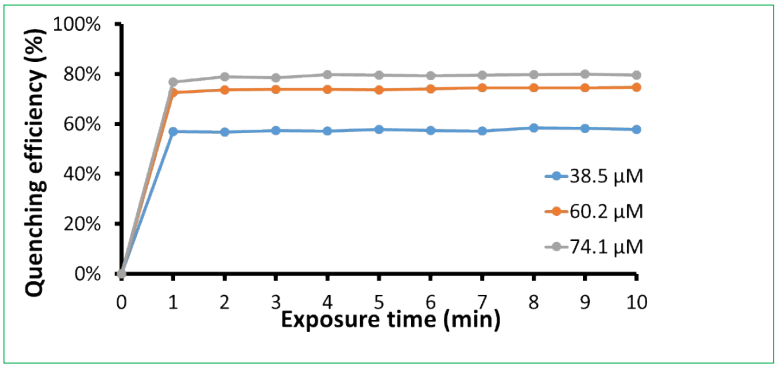

Fig. S21. Exposure time experiment of **TBNap-TPy** in DMSO-H_2O (70-30) (c= $4.6x10^{-6}$ M) in the presence of different concentrations of PA.

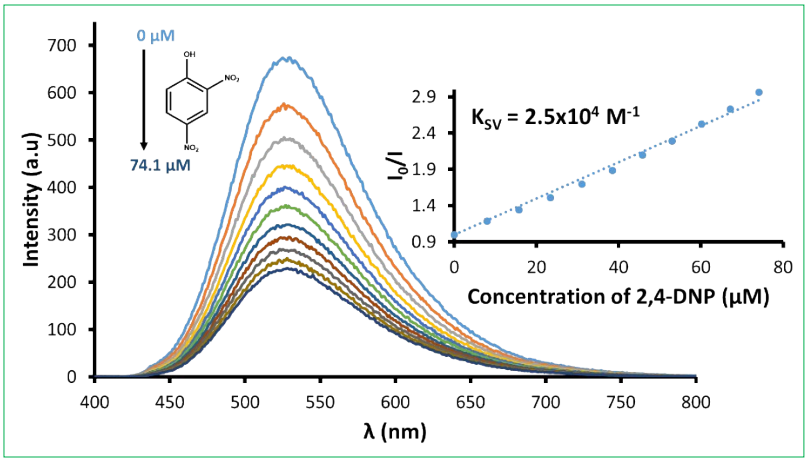

Fig. S22. Observed fluorescence quenching of **TBNap-TPy** upon addition of 2,4-DNP in DMSO-H_2O (70-30) (insert: Stern-Volmer plot).

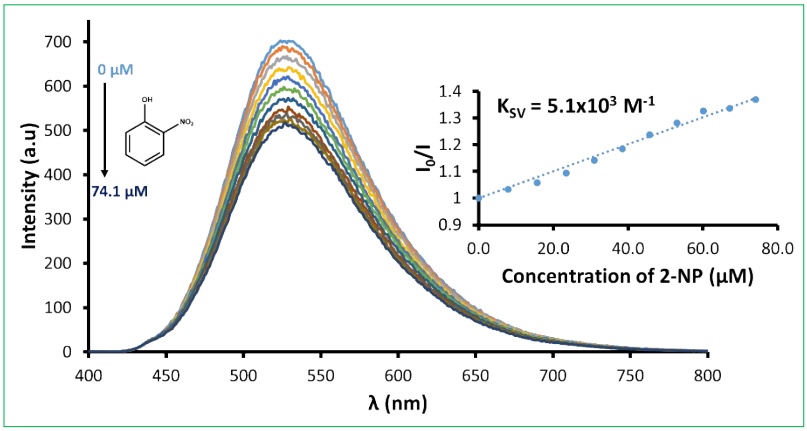

Fig. S23. Observed fluorescence quenching of **TBNap-TPy** upon addition of 2-NP in DMSO-H_2O (70-30) (insert: Stern-Volmer plot).

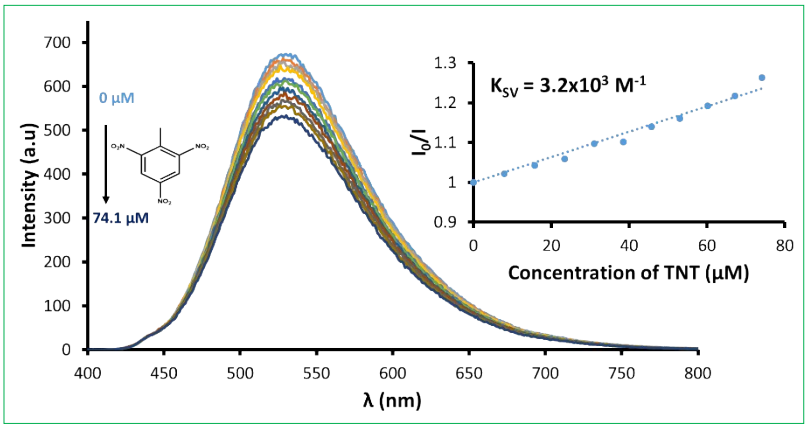

Fig. S24. Observed fluorescence quenching of **TBNap-TPy** upon addition of TNT in DMSO-H_2O (70-30) (insert: Stern-Volmer plot).

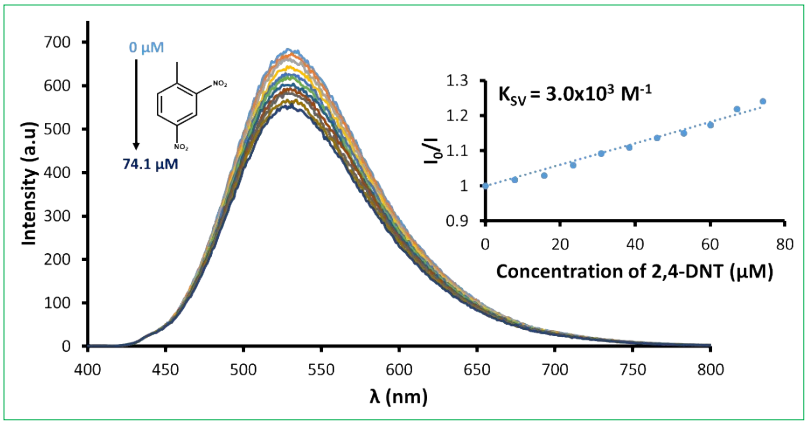

Fig. S25. Observed fluorescence quenching of **TBNap-TPy** upon addition of 2,4-DNT in DMSO-H_2O (70-30) (insert: Stern-Volmer plot).

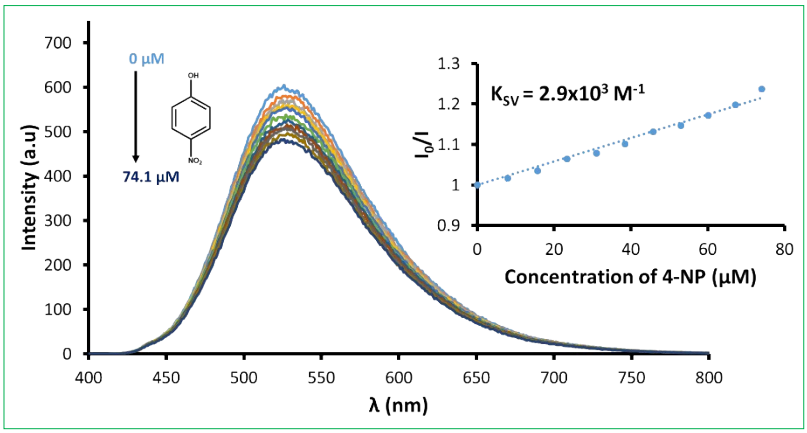

Fig. S26. Observed fluorescence quenching of **TBNap-TPy** upon addition of 4-NP in DMSO-H_2O (70-30) (insert: Stern-Volmer plot).

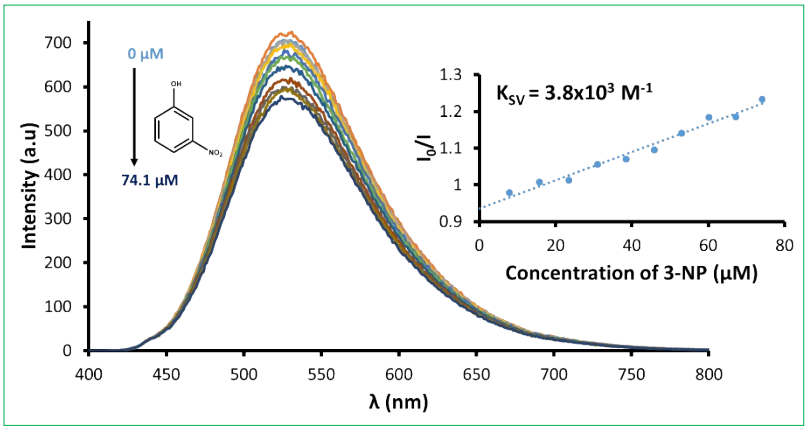

Fig. S27. Observed fluorescence quenching of **TBNap-TPy** upon addition of 3-NP in DMSO-H_2O (70-30) (insert: Stern-Volmer plot).

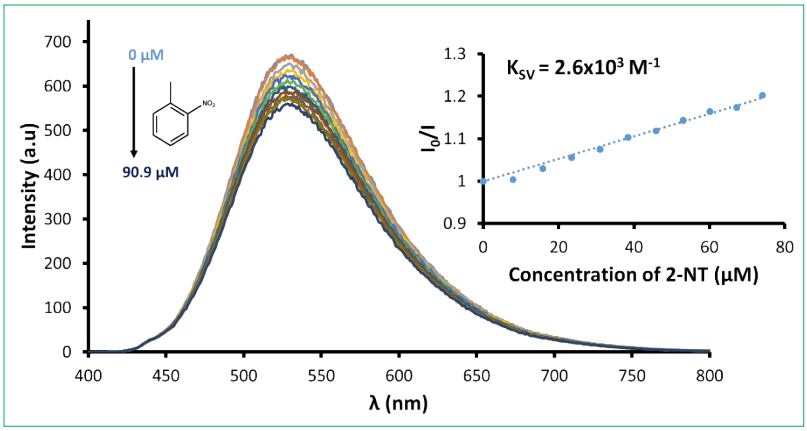

Fig. S28. Observed fluorescence quenching of **TBNap-TPy** upon addition of 2-NT in DMSO-H_2O (70-30) (insert: Stern-Volmer plot).

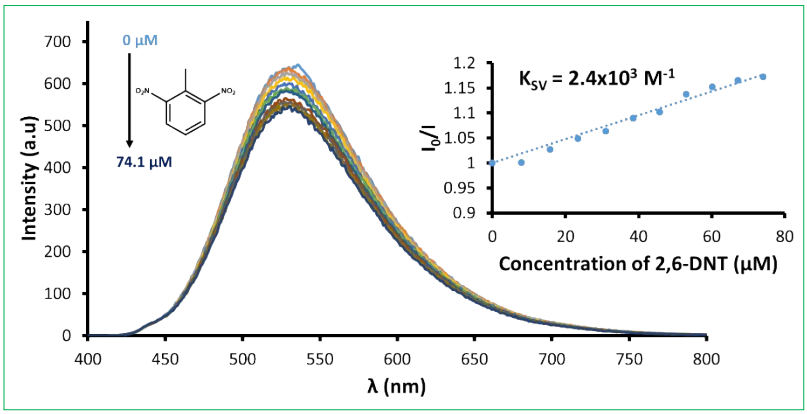

Fig. S29. Observed fluorescence quenching of **TBNap-TPy** upon addition of 2,6-DNT in DMSO-H_2O (70-30) (insert: Stern-Volmer plot).

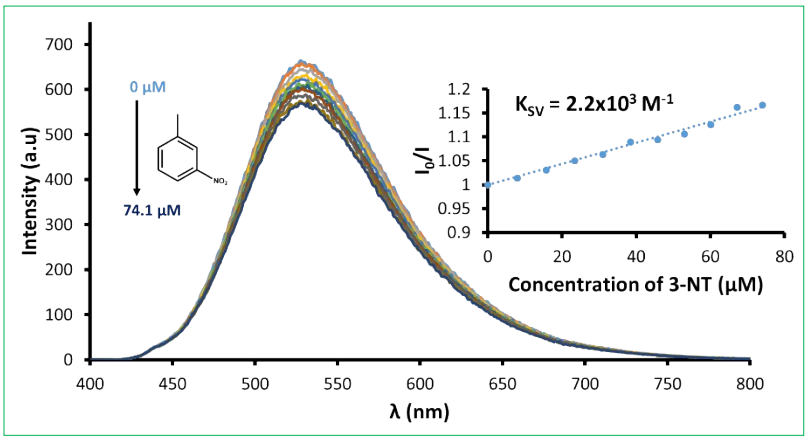

Fig. S30. Observed fluorescence quenching of **TBNap-TPy** upon addition of 3-NT in DMSO-H_2O (70-30) (insert: Stern-Volmer plot).

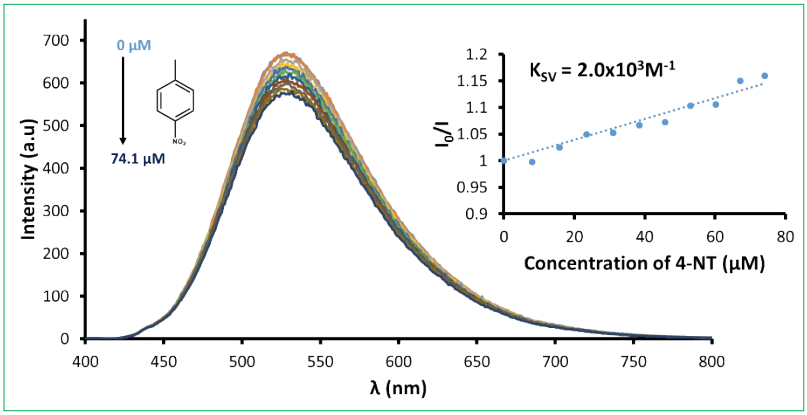

Fig. S31. Observed fluorescence quenching of **TBNap-TPy** upon addition of 4-NT in DMSO-H_2O (70-30) (insert: Stern-Volmer plot).

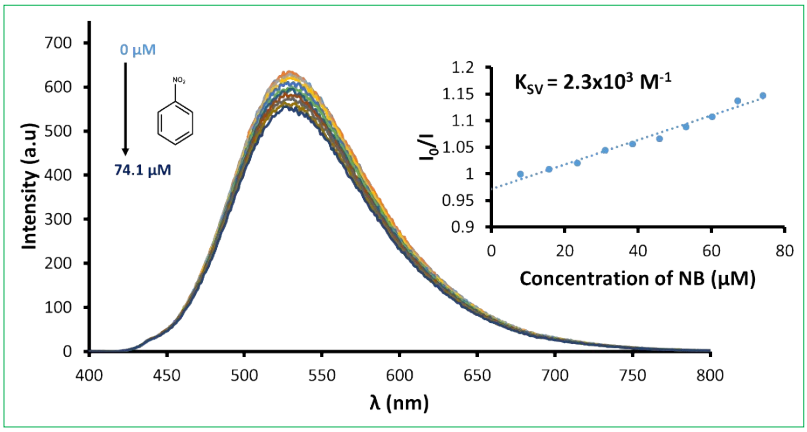

Fig. S32. Observed fluorescence quenching of **TBNap-TPy** upon addition of NB in DMSO-H_2O (70-30) (insert: Stern-Volmer plot).

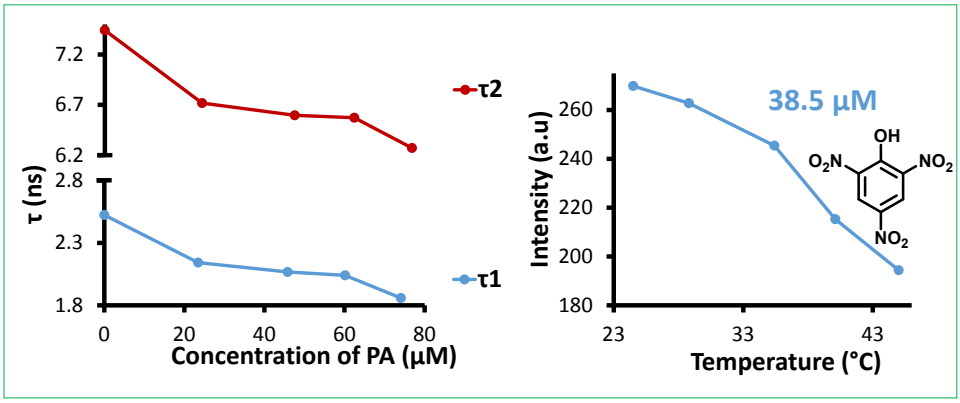

Fig. S33. The fluorescence decay profiles of **TBNap-TPy** upon addition of PA (0-74 µM) (left) and its temperature-dependent emission profile in the presence of PA (38.5 µM) (right).

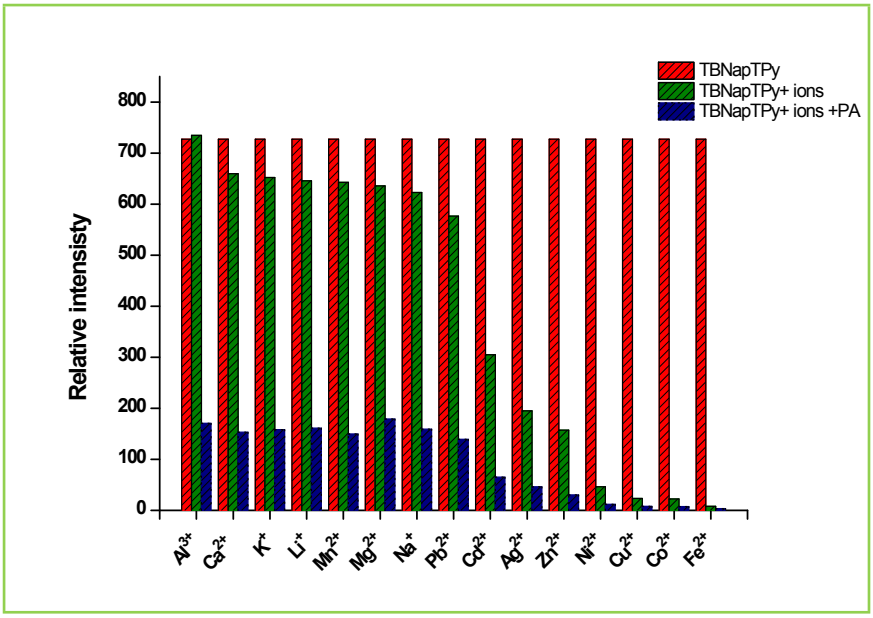

Fig. S34. The competitive selective affinity of **TBNap-TPy** (c = 4.6 × 10^{-6} M) towards PA in the presence and absence of different metal cations in DMSO-H_2O (70-30%) mixture.

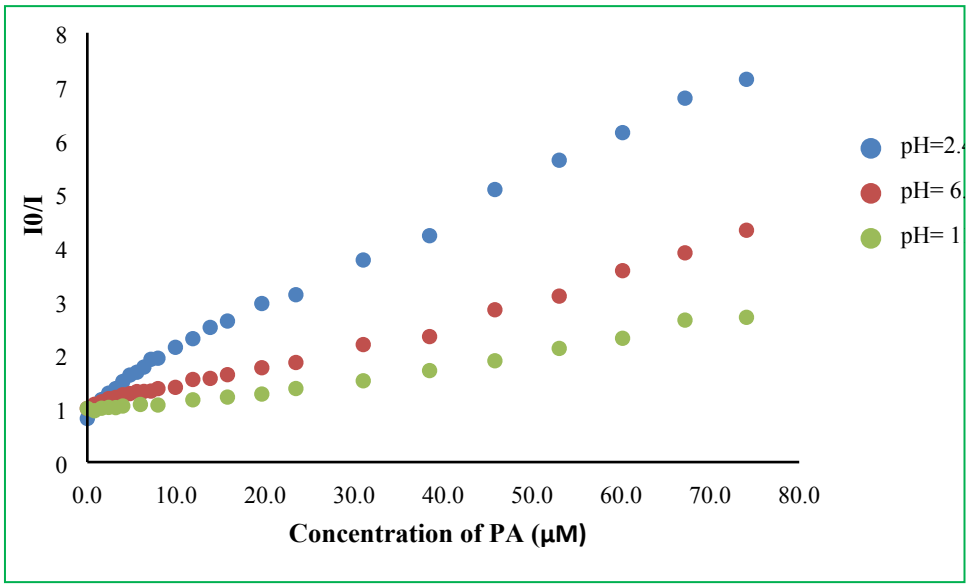

Fig. S35. Relative changes in emission intensity of **TBNap-TPy** towards PA in DMSO-H_2O (1-99%) mixture at different pH = 2.4 to 11 of the medium.

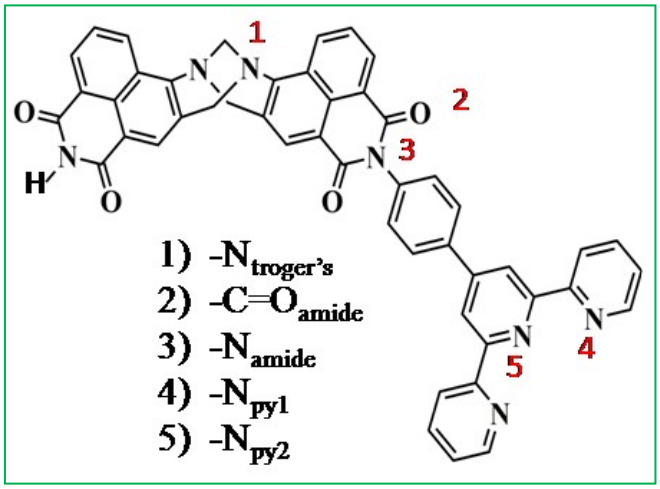

Fig. S36.The model system used to represent **TBNap-TPy** and possible sites of interactions with PA.

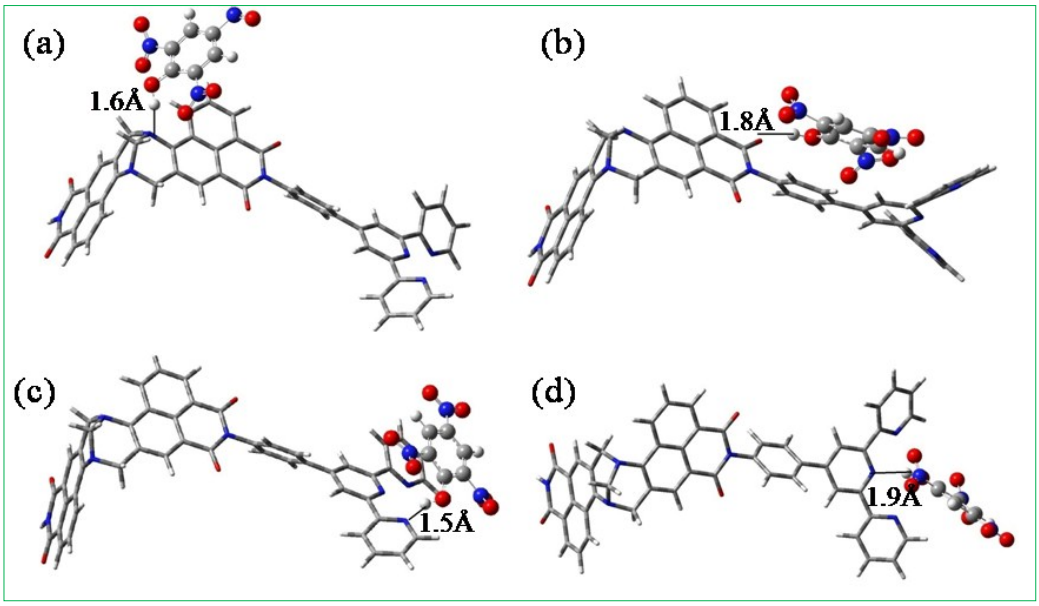

Fig. S37. Optimized structures, nearest intermolecular distances of the **TBNap-TPy** complexes with PA at (a) -$N_{Tröger's}$ (b) -C=O_{imide} (c) -N_{Py1} and (d) -N_{Py2} sites. (The structure of **TBNap-TPy** is given in tube representation for clarity).

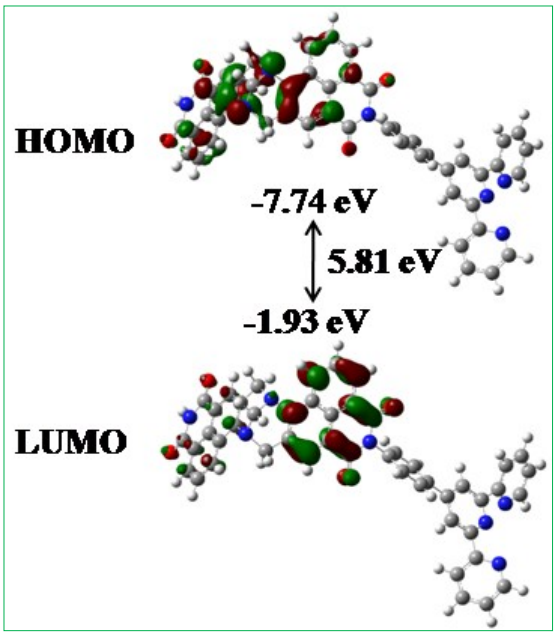

Fig. S38. Frontier molecular orbital with their corresponding energy values, for the **TBNap-TPy** model system.

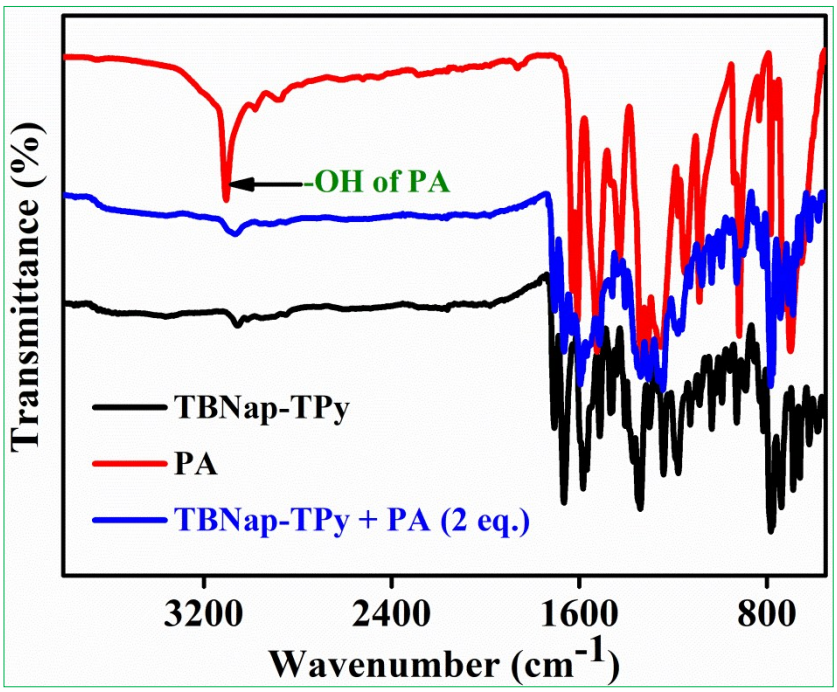

Fig. S39. FT-IR spectra of PA, and **TBNap-TPy** before and after the mixing of PA.

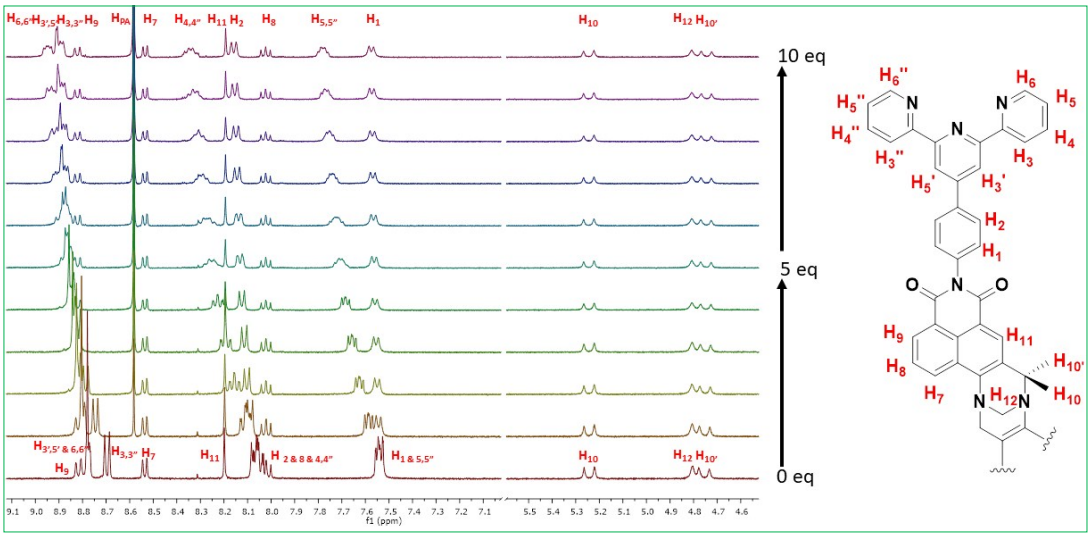

Fig. S40. The change in ^{1}H NMR of spectra (400 MHz, DMSO-d_6) of **TBNap-TPy** upon mixing picric acid at a gradual increase in concentration over 0.0→10 equivalents.